PERFORMANCE EVALUATION OF CFRP-RETROFITTED CIRCULAR T-JOINTS UNDER DAMAGE AND ELEVATED TEMPERATURE CONDITIONS

Prof. Dr. S. M. Zahurul Islam[1], Faruque Abdullah*[2], Tasbirul Hussain[3] and Salma Anika[4]

[1] *Professor, Rajshahi University of Engineering & Technology, Bangladesh, e-mail: zahurul90@gmail.com*
[2] *Assistant Professor, Rajshahi University of Engineering & Technology, Bangladesh, e-mail: abdullahruet13@gmail.com*
[3] *Lecturer, European University of Bangladesh, Dhaka, Bangladesh, e-mail: opu.hussain547@gmail.com*
[4] *Student, Rajshahi University of Engineering & Technology, Bangladesh, e-mail: salmaanika09@gmail.com*

***Corresponding Author**

ABSTRACT

This study investigates the structural performance of circular hollow section T-joints (CHST–CHST) retrofitted with Carbon Fiber Reinforced Polymer (CFRP) under varying levels of damage, fiber orientations, and temperature conditions. Twenty specimens were tested, including undamaged, one-sided, and bilaterally degraded joints with 2-inch and 3-inch chord wall cuts, strengthened with CFRP at orientations of 0°, 45°, and 90°. Results show that CFRP retrofitting significantly enhances load-carrying capacity and ductility in moderately damaged joints by delaying failure and improving energy absorption, while its effectiveness diminishes with increasing severity of degradation. Elevated temperatures further reduced joint performance, as adhesive and matrix degradation limited the contri-bution of CFRP despite the steel retaining most of its strength. CFRP reinforce-ment proves to be an effective method for enhancing the resilience and extending the service life of circular tubular joints, although its benefits are limited by severe damage and elevated temperatures.

Keywords: *CFRP, Circular hollow steel section (CHSS), T-joint, Retrofitting.*

1. INTRODUCTION

Hollow steel sections (HSS) are commonly employed in steel construction because of their superior strength-to-weight efficiency. However, since they are composed of thin plate elements, these sections are prone to local buckling under axial compression before the steel attains its yield strength (Shi, Wang, et al., 2014; Shi, Zhou, et al., 2014). However, the most critical part of HSS structure is joint and hence the structure is collapsed. For the case of T-joints it is susceptible to deterioration, overloading and sometimes for accidental impacts (Aguilera & Fam, 2013; Deng et al., 2019; Fu et al., 2016). That's why these joints are recognized as the most critical and weakest components in tubular structural systems (Qu et al., 2014). To overcome this threat some common reinforcement techniques for tubular joints such as the use of external stiffeners (Li et al., 2018; Zhu et al., 2017), internal ring stiffeners (Lee & Llewelyn-Parry, 2004), partially thickened chord walls (Yang et al., 2012), double plate reinforcements (Choo et al., 2004; Fung et al., 1999; Nassiraei et al., 2016), and collar plates (Qu et al., 2017) are in common practices. There are some disadvantages on using these traditional techniques like as the application of steel plates for strengthening HSS joints often leads to an increased dead load and welding-induced fatigue, which has driven the shift toward FRP-based solutions (Karbhari & Shulley, 1995).

At presents, most of the strengthening techniques using CFRP has been introduced on concrete structures and only a limited investigation performed on steel tubular joints to assess the effectiveness of CFRP. Besides this, due to the superior strength, durability and resistance to environmental degradation the tendency of using CFRP on steel reinforcement is increasing to improve the load carrying performance and as well as ductility (Islam et al., 2019; Sadat Hosseini et al., 2020; Tafsirojjaman et al., 2021). Experimental research on the application of CFRP on metallic structure as well as numerical analysis of FRP strengthen steel tubular T-joints has shown a remarkable enhancement in ultimate strength and overall joint performance (Lesani et al., 2013). Addition of one more layer on the previous CFRP strips on the tension flanges of steel beam shows an approximately 40% increase in load carrying capacity (Colombi & Poggi, 2006). Slender steel square columns subjected to axial loading and transversely wrapped with three layers of CFRP at a b/t ratio of 100 exhibited up to a 31% increase in axial strength (Park et al., 2013). The effectiveness of FRP confinement has been validated through studies focused on strengthening various steel elements, particularly beams (Ghafoori et al., 2012a, 2012b; Ghafoori & Motavalli, 2013). Experimental investigations and finite element analyses have shown that CFRP sheets can carry up to half of the joint's load, significantly enhance joint strength compared to unreinforced specimens, and effectively delay plastic failure of the chord surface (Lesani et al., 2013, 2014, 2015). Cracked alumi-num connections retrofitted with GFRP under static loading achieved load capacities ranging from 117% to 125% of those observed in welded connections with comparable crack lengths (Pantelides et al., 2003).

Although the research on the effectiveness of CFRP in strengthening steel T-joints is satisfactory but limited attention has been given on the effectiveness of retrofitting on HSS T-joints under different degrees of damages. This study investigated the performance of CFRP retrofitted HSS tubular joints focusing on the effect of damage condition at the chord wall.

2. EXPERIMENTAL FRAMEWORK

Twenty steel hollow steel T-joints were prepared for the study. All of these specimens consisted of both chord and web sections made from Circular Hollow Steel Tubes (CHST). All the geometric details (Length, width and height or diameter for circular section) has been included in Table 1. Each specimen name is uniquely lebelled with a systematic coding scheme that represents the section property, fiber orientation and degradation length. The first two letters "CC" refers to both chord and web being circular cross-section in geometry. The numerical digits "1S" or "2S" that follow these letters denote the extent of chord wall degradation: "1S" represents degradation on one side of the chord wall, while "2S" signifies degradation on both sides. Additionally, the letters "A" or "B" specify the length of the wall degradation, corresponding to 2 inches and 3 inches respectively as well as the thickness is 1.23 mm for all the samples. Finally, the numbers "0", "45", and "90" refer to the

orientation angles of the externally bonded CFRP, measured in degrees relative to the longitudinal axis of the web member.

Table 1: Geometric properties of CFRP-strengthened steel T-joint specimens.

Sl. No.	Specimen Name	Chord			Web		
		L_0 (mm)	D_0 (mm)	t_0 (mm)	L_1 mm)	D_1 (mm)	t_1 (mm)
1.	CC1SA	305	90	2.9	117	59	2.9
2.	CC1SA0	303	90	2.9	117	59	2.9
3.	CC1SA45	305	90	2.9	119	59	2.9
4.	CC1SA90	308	90	2.9	114	59	2.9
5.	CC1SB	305	90	2.9	116	59	2.9
6.	CC1SB0	305	90	2.9	114	59	2.9
7.	CC1SB45	305	90	2.9	117	59	2.9
8.	CC1SB90	305	90	2.9	112	59	2.9
9.	CC2SA	308	90	2.9	118	59	2.9
10.	CC2SA0	305	90	2.9	115	59	2.9
11.	CC2SA45	305	90	2.9	116	59	2.9
12.	CC2SA 90	305	90	2.9	117	59	2.9
13.	CC2SB	304	90	2.9	120	59	2.9
14.	CC2SB0	303	90	2.9	120	59	2.9
15.	CC2SB45	303	90	2.9	119	59	2.9
16.	CC2SB90	305	90	2.9	118	59	2.9
17.	TCC25	304	90	2.9	121	59	2.9
18.	TCC100	305	90	2.9	118	59	2.9
19.	TCC200	305	90	2.9	117	59	2.9
20.	TCC300	303	90	2.9	120	59	2.9

Across all 20 specimens in this table, both the chord and web sections maintain consistent diameters of 90 mm and 59 mm respectively, with a uniform wall thickness of 2.9 mm. The chord lengths range slightly from 303 mm to 308 mm and in case of web lengths it varies from 112 mm to 121 mm. Additionally, the samples that does not include any digit used for comparing the performance of CFRP on different cases for each sector. For this case, three test samples are used for comparing the strength behavior at moderate temperatures. The name "TCC" refers to a test specimen where we used both the chord and web are circular in cross section. The digit following "TCC" indicates the temperature at which the samples were kept in the oven for 15 minutes. For these samples the CFRP orientation was 90° and are free from any intentional damaged. An additional specimen labeled "TCC" not included in the table, was prepared without CFRP or degradation to serve as a baseline for evaluating load reduction or increment as a result of retrofiting on the samples of varying damage levels. The length, diameter and thickness of chord is 305 mm, 90 mm and 2.9 mm respectively and for the web section it is 120 mm, 59 mm and 2.9 mm respectively for the sample TCC.

The structural reinforcement system employed in this study consists of an epoxy adhesive and a unidirectional carbon fiber fabric, each contributing distinct mechanical properties. The epoxy adhesive, with a density of 1.80 ± 0.1 kg/L, provides strong adhesion and exhibits tensile strengths of ≥ 5 N/mm² after 3 days and ≥ 8 N/mm² after 7 days, along with a tensile modulus of 1500 MPa. Its elongation at break is limited to 0.28%, indicating high rigidity, and it performs effectively within a temperature range of +10°C to +40°C. In contrast, the carbon fiber fabric possesses a higher density of 1.82 g/cm³, a tensile strength of 4,000 N/mm², and a significantly greater modulus of elasticity of 230,000 N/mm². Its elongation at break reaches 1.7%, offering improved flexibility relative to the epoxy. The high-strength steel used in the specimens has a yield strength (fy) of 470 MPa and an ultimate tensile strength (fu) of 507 MPa, with corresponding yield and ultimate strains of 0.64% and 27.5%, respectively.

During the compressive loading tests on steel T-joints, Linear Variable Differential Transformers (LVDTs) were strategically positioned to capture deformation responses at critical locations. Two LVDTs were mounted on opposite sides of the joint to measure vertical displacement under axial compression.

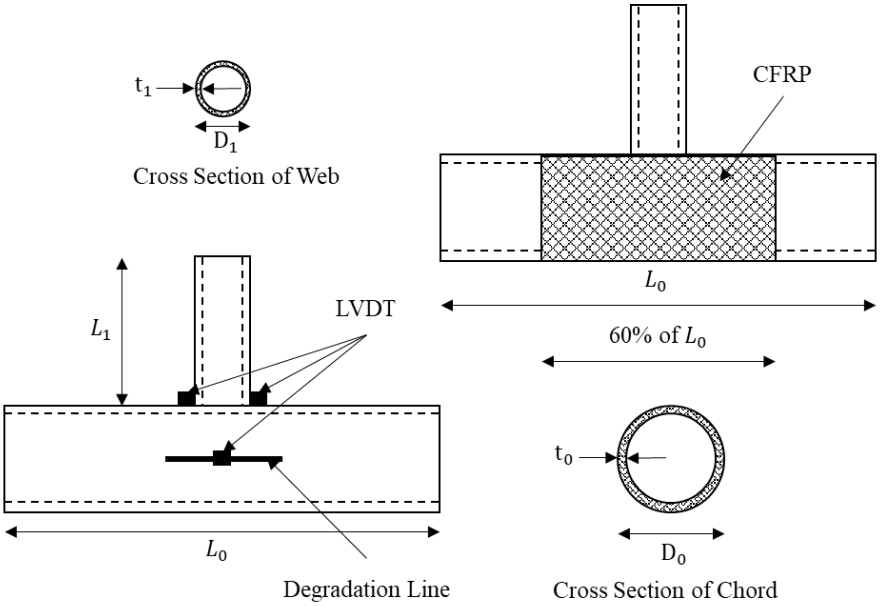

Figure 1: Geometry and loading condition of test specimen.

In the compressive load test on steel T-joints, the Linear Variable Differential Transformers (LVDTs) are strategically placed to monitor the deformation of the specimen at different locations as shown in Figure 1. Two LVDT is positioned directly on the joint of the steel T-joint in two opposite sides to measure the vertical displacement or deformation occurring at the joint under the applied compressive load and average of the both reading was counted in reports. Both side of the sample was free boundary condition and the bottom rests on the plate. Besides the geometric details and CFRP rapping length has been represented in Figure 1.

3. TEST RESULTS AND DISCUSSION

This analysis examines the structural behaviour of steel T-joints under varying degrees of damage and their subsequent rehabilitation using CFRP strengthening. The T-joint in Figure 2(a) and 2(c) has a 2-inch and 3-inch crack along one chordal side respectively. Localized damage diminishes the load-carrying capacity of a steel joint between a circular tube chord and a circular tube web. Applying CFRP for retrofitting counteracts this by delaying failure, thus boosting performance well above the damaged level (load carrying capacity enhancement performance is 24.01% and 15.56% and ductility enhancement performance is 25.69% and 14.39% respectively for 2-inch and 3-inch damaged sample for 90-degree Orientation).

Despite this improvement, the retrofitted joint cannot match the performance of the original, undamaged structure. In the more severe scenario Figure 2(b) & 2(d), a 3-inch damage affects a joint composed entirely of CHST members. The increased damage length critically weakens the joint by compromising a larger structural area, which results in a pronounced reduction in load-carrying capacity and a higher vulnerability to failure. Consequently, while CFRP retrofitting is projected to yield a greater performance enhancement (load carrying capacity and ductility enhancement performance is 34.84% and 19.73% but the ductility did not increase too much like as 7.65% and 8.89% respectively 2-inch and 3-inch damaged sample for 90-degree Orientation). This bilateral damage creates a highly degraded state, severely compromising the joint's axial load resistance and drastically reducing its load-carrying capacity. While CFRP strengthening cannot fully restore the

joint to its original strength, it is crucial for mitigating performance loss, preventing immediate failure, and extending service life.

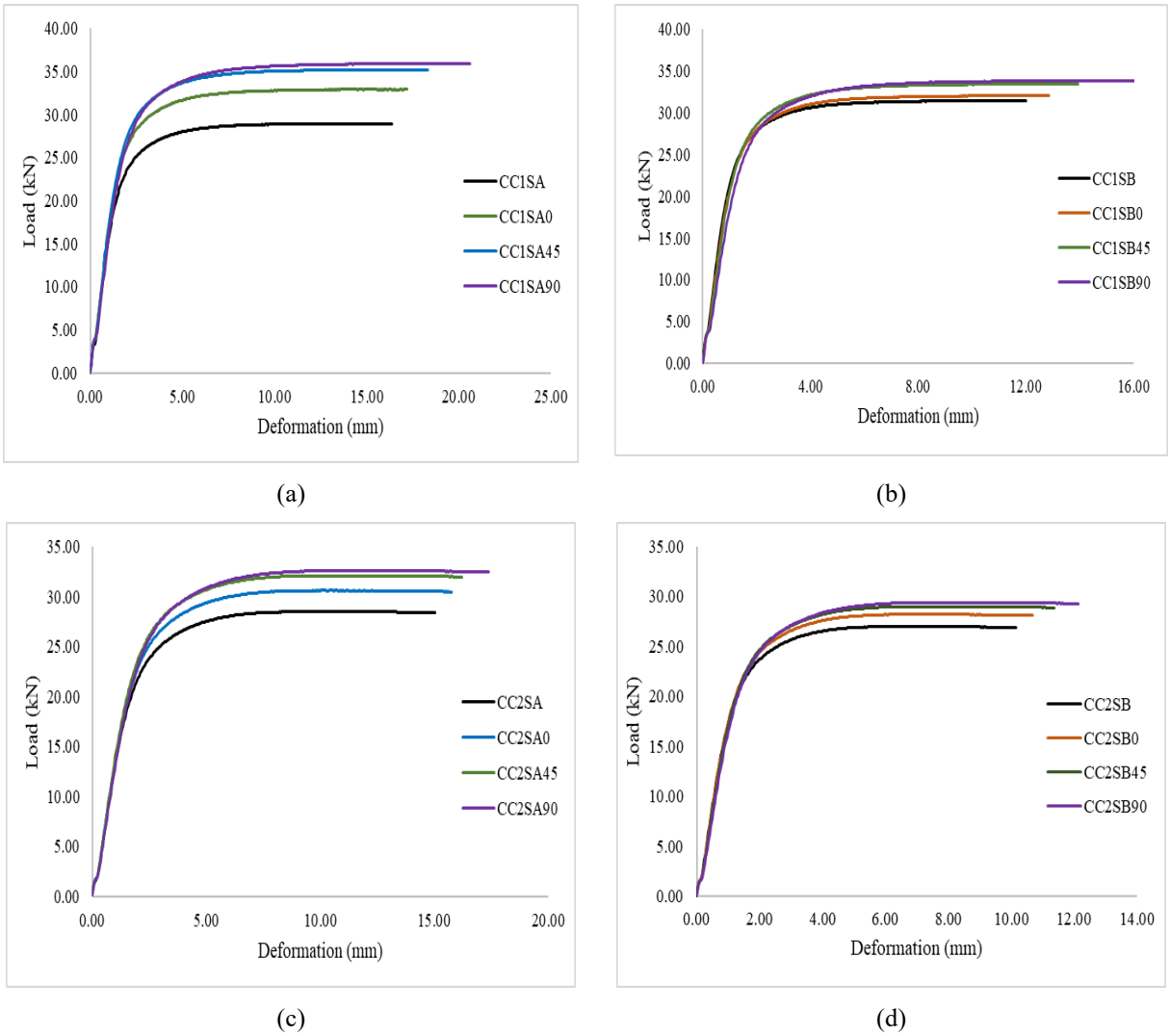

Figure 2: Load carrying capacity of T-joint; (a) One side 2-inch damage; (b) One side 3-inch damage; (c) Two side 2-inch damage and (d) Two side 3-inch damage.

A significant and non-linear degradation in load-carrying capacity with increasing temperature as shown in Figure 3. At an ambient temperature of 25°C, the CFRP-retrofitted joint sustains a peak load of 42.0 kN. Compared to the steel joint sample without damaged and without retrofitting sample TCC (capacity 29.9 kN) there is an increment of 40.47% in peak load capacity. However, with the increasing temperature the capacity declines significantly up to a certain temperature. At 100°C temperature the polymer of epoxy adhesive begins to soften and exceed its glass transition temperature. So the load capacity reduced to 35. kN at this level of temperature. This downward trend continues as a result of breakdown of the adhesive integrity due to rise of temperature and hence affect the CFRP matrix. At 200°C, the joint can withstand only 29.4 kN. After this temperature the role of CFRP almost destroyed and so the trend is not linear after this temperature. By 300°C, the capacity lowered to 28.0 kN. From this data it is clear that at elevated temperatures the effectiveness of the CFRP is questionable. At this stage, compared to TCC the sample loses nearly 6.35% of its initial strength. The primary driver of this failure is not steel at all, which retains most of its strength up to 300°C temperature. The thermal degradation of polymer adhesive and composite matrix a cause of bond failure and a loss of composite action before the steel starts losing its strength.

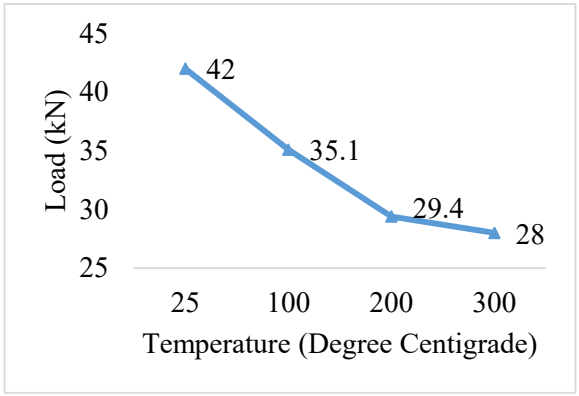

Figure 3: Temperature effect on CFRP strengthened steel T-Joints.

A study on the effectiveness of CFRP retrofitting for steel T-joints with varying types and degree of degradation is presented in the Figure 4, with all specimens tested at 90-degree orientation. The graph shows the load carrying capacity in four different cases which directly linked with the initial damage condition. The CHST-CHST steel T-joints with a single side 2-inch initial damaged sample exhibits the highest load capacity as well as ductility property corresponding to ultimate loading. The main mechanism behind the increment is the restored stiffness due to addition of CFRP retrofitting which allows the joint to sustained plastic deformation before failure. All the samples with 3-inch initial damaged in one side or both side bears lower load compared to 2-inch damages. In this case it denotes that with increasing the crack length the effectiveness of CFRP is limited. As a result, the CFRP absorb lower energy and less pronounced yield plateau. In case of two side 3-inch damage the scenario is more critical in both load capacity and ductility behaviour. Thus the situation leads to a brittle failure mechanism with minimal deformation. So it can be concluding that the effectiveness in enhancing structural performance is constrained by the extent of the initial damage.

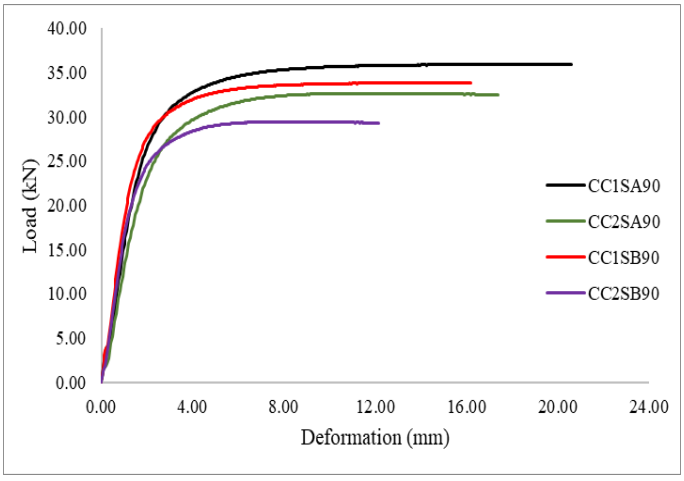

Figure 4: Load carrying capacity of Steel T-joint at orientation for different degradation.

4. CONCLUSIONS

This study evaluated the structural behaviour of circular tubular T-joints strengthened with CFRP under different damage conditions and temperatures. The findings show that CFRP retrofitting

significantly improves load-carrying capacity and ductility, particularly in specimens with minor degradation, where confinement effectively delayed failure and enhanced energy absorption.

The extent of initial damage was found to be a key factor, with one-sided 2-inch cracks showing the highest gains, while bilaterally damaged joints exhibited limited improvement, indicating that CFRP effectiveness decreases as damage severity in-creases. Temperature also played a critical role: although CFRP performed well at ambient conditions, elevated temperatures led to progressive strength loss due to adhesive and matrix degradation, rather than weakening of the steel itself.

DECLARATION OF USE OF AI

The authors declare that no artificial intelligence (AI) tools or technologies were used in the preparation, writing, analysis, or revision of this manuscript. All content, including the research design, data analysis, interpretation of results, and manuscript writing, was carried out only by the authors.

REFERENCES

Aguilera, J., & Fam, A. (2013). Retrofitting tubular steel T-joints subjected to axial compression in chord and brace members using bonded FRP plates or through-wall steel bolts. Engineering Structures, 48, 602–610. https://doi.org/10.1016/j.engstruct.2012.09.018

Choo, Y. S., Liang, J. X., Van Der Vegte, G. J., & Liew, J. Y. R. (2004). Static strength of doubler plate reinforced CHS X-joints loaded by in-plane bending. Journal of Constructional Steel Research, 60(12), 1725–1744. https://doi.org/10.1016/j.jcsr.2004.05.004

Colombi, P., & Poggi, C. (2006). An experimental, analytical and numerical study of the static behavior of steel beams reinforced by pultruded CFRP strips. Compo-sites Part B: Engineering, 37(1), 64–73. https://doi.org/10.1016/j.compositesb.2005.03.002

Deng, P., Guo, J., Liu, Y., & Wang, Z. (2019). Compressive Behavior of Damaged Tubular T-joints Retrofitted with Collar Plate. KSCE Journal of Civil Engineering, 23(9), 4085–4101. https://doi.org/10.1007/s12205-019-0276-y

Fu, Y., Tong, L., He, L., & Zhao, X.-L. (2016). Experimental and numerical investi-gation on behavior of CFRP-strengthened circular hollow section gap K-joints. Thin-Walled Structures, 102, 80–97. https://doi.org/10.1016/j.tws.2016.01.020

Fung, T. C., Chan, T. K., & Soh, C. K. (1999). Ultimate Capacity of Doubler Plate–Reinforced Tubular Joints. Journal of Structural Engineering, 125(8), 891–899. https://doi.org/10.1061/(ASCE)0733-9445(1999)125:8(891)

Ghafoori, E., & Motavalli, M. (2013). Flexural and interfacial behavior of metallic beams strengthened by prestressed bonded plates. Composite Structures, 101, 22–34. https://doi.org/10.1016/j.compstruct.2013.01.021

Ghafoori, E., Schumacher, A., & Motavalli, M. (2012a). Fatigue behavior of notched steel beams reinforced with bonded CFRP plates: Determination of prestress-ing level for crack arrest. Engineering Structures, 45, 270–283. https://doi.org/10.1016/j.engstruct.2012.06.047

Ghafoori, E., Schumacher, A., & Motavalli, M. (2012b). Fatigue behavior of notched steel beams reinforced with bonded CFRP plates: Determination of prestress-ing level for crack arrest. Engineering Structures, 45, 270–283. https://doi.org/10.1016/j.engstruct.2012.06.047

Islam, S. M. Z., Cai, Y., & Young, B. (2019). Design of CFRP-strengthened stain-less steel tubular sections subjected to web crippling. Journal of Constructional Steel Research, 159, 442–458. https://doi.org/10.1016/j.jcsr.2019.04.043

Karbhari, V. M., & Shulley, S. B. (1995). Use of Composites for Rehabilitation of Steel Structures—Determination of Bond Durability. Journal of Materials in Civil Engineering, 7(4), 239–245. https://doi.org/10.1061/(ASCE)0899-1561(1995)7:4(239)

Lee, M. M. K., & Llewelyn-Parry, A. (2004). Offshore Tubular T-Joints Reinforced with Internal Plain Annular Ring Stiffeners. Journal of Structural Engineering, 130(6), 942–951. https://doi.org/10.1061/(ASCE)0733-9445(2004)130:6(942)

Lesani, M., Bahaari, M. R., & Shokrieh, M. M. (2013). Numerical investigation of FRP-strengthened tubular T-joints under axial compressive loads. Composite Struc-tures, 100, 71–78. https://doi.org/10.1016/j.compstruct.2012.12.020

Lesani, M., Bahaari, M. R., & Shokrieh, M. M. (2014). Experimental investigation of FRP-strengthened tubular T-joints under axial compressive loads. Construction and Building Materials, 53, 243–252. https://doi.org/10.1016/j.conbuildmat.2013.11.097

Lesani, M., Bahaari, M. R., & Shokrieh, M. M. (2015). FRP wrapping for the reha-bilitation of Circular Hollow Section (CHS) tubular steel connections. Thin-Walled Structures, 90, 216–234. https://doi.org/10.1016/j.tws.2014.12.013

Li, W., Zhang, S., Huo, W., Bai, Y., & Zhu, L. (2018). Axial compression capacity of steel CHS X-joints strengthened with external stiffeners. Journal of Constructional Steel Research, 141, 156–166. https://doi.org/10.1016/j.jcsr.2017.11.009

Nassiraei, H., Lotfollahi-Yaghin, M. A., & Ahmadi, H. (2016). Static performance of doubler plate reinforced tubular T/Y-joints subjected to brace tension. Thin-Walled Structures, 108, 138–152. https://doi.org/10.1016/j.tws.2016.08.012

Pantelides, C. P., Nadauld, J., & Cercone, L. (2003). Repair of Cracked Aluminum Overhead Sign Structures with Glass Fiber Reinforced Polymer Composites. Journal of Composites for Construction, 7(2), 118–126. https://doi.org/10.1061/(ASCE)1090-0268(2003)7:2(118)

Park, J.-W., Yeom, H.-J., & Yoo, J.-H. (2013). Axial loading tests and FEM analysis of slender square hollow section (SHS) stub columns strengthened with carbon fiber reinforced polymers. International Journal of Steel Structures, 13(4), 731–743. https://doi.org/10.1007/s13296-013-4014-x

Qu, H., Huo, J., Xu, C., & Fu, F. (2014). Numerical studies on dynamic behavior of tubular T-joint subjected to impact loading. International Journal of Impact Engi-neering, 67, 12–26. https://doi.org/10.1016/j.ijimpeng.2014.01.002

Qu, H., Li, A., Huo, J., & Liu, Y. (2017). Dynamic performance of collar plate rein-forced tubular T-joint with precompression chord. Engineering Structures, 141, 555–570. https://doi.org/10.1016/j.engstruct.2017.03.037

Sadat Hosseini, A., Bahaari, M. R., & Lesani, M. (2020). Experimental and para-metric studies of SCFs in FRP strengthened tubular T-joints under axially loaded brace. Engineering Structures, 213, 110548. https://doi.org/10.1016/j.engstruct.2020.110548

Shi, G., Wang, J., Bai, Y., & Shi, Y. (2014). Experimental Study on Seismic Behav-ior of 460MPa High Strength Steel Box-Section Columns. Advances in Structural Engineering, 17(7), 1045–1059. https://doi.org/10.1260/1369-4332.17.7.1045

Shi, G., Zhou, W., Bai, Y., & Lin, C. (2014). Local buckling of 460MPa high strength steel welded section stub columns under axial compression. Journal of Con-structional Steel Research, 100, 60–70. https://doi.org/10.1016/j.jcsr.2014.04.027

Tafsirojjaman, T., Fawzia, S., & Thambiratnam, D. P. (2021). Structural behaviour of CFRP strengthened beam-column connections under monotonic and cyclic load-ing. Structures, 33, 2689–2699. https://doi.org/10.1016/j.istruc.2021.06.028

Yang, J., Shao, Y., & Chen, C. (2012). Static strength of chord reinforced tubular Y-joints under axial loading. Marine Structures, 29(1), 226–245. https://doi.org/10.1016/j.marstruc.2012.06.003

Zhu, L., Song, Q., Bai, Y., Wei, Y., & Ma, L. (2017). Capacity of steel CHS T-Joints strengthened with external stiffeners under axial compression. Thin-Walled Struc-tures, 113, 39–46. https://doi.org/10.1016/j.tws.2017.01.007